

Strontium-containing nanostructured hydroxyapatite microspheres for bone regeneration

Microesferas de hidroxiapatita nanoestruturada substituída por estrôncio para regeneração óssea

Microesferas de hidroxiapatita nanoestruturadas sustituidas con estroncio para la regeneración ósea

Received: 03/27/2023 | Revised: 04/09/2023 | Accepted: 04/10/2023 | Published: 04/15/2023

Iorrana Índira dos Anjos Ribeiro

ORCID: <https://orcid.org/0000-0002-9602-1708>

Universidade Federal da Bahia, Brasil

E-mail: indiraanjos@gmail.com

Aryon de Almeida Barbosa Júnior

ORCID: <https://orcid.org/0000-0001-6210-2107>

Instituto de Patologia Cutânea, Brasil

E-mail: ary3on@hotmail.com

Alexandre Malta Rossi

ORCID: <https://orcid.org/0000-0003-4244-8455>

Centro Brasileiro de Pesquisas Físicas, Brasil

E-mail: alex.mrossi@gmail.com

Renata dos Santos Almeida

ORCID: <https://orcid.org/0000-0001-8359-6345>

Universidade Federal da Bahia, Brasil

E-mail: renata.almeidabio@gmail.com

Fúlvio Borges Miguel

ORCID: <https://orcid.org/0000-0002-0607-0208>

Universidade Federal da Bahia, Brasil

E-mail: fulviomiguel@ufba.br

Fabiana Paim Rosa

ORCID: <https://orcid.org/0000-0002-3731-2177>

Universidade Federal da Bahia, Brasil

E-mail: fabianapaim@hotmail.com

Abstract

The aim of this study was to analyze the biological behavior and osteogenic potential of nanostructured hydroxyapatite microspheres substituted with strontium (nHASr). Therefore, twenty adult male Wistar rats were randomly distributed into two groups: GnHASr – critical bone defect filled with nHASr microspheres; e CG (control group) – critical bone defect without implantation of biomaterial; evaluated at the biological points of 30 and 60 days. The collected specimens were processed and stained with hematoxylin-eosin (HE) and Masson-Goldner trichrome (TG) and examined by light microscopy. Posteriorly, they were analyzed histomorphometrically to measure the percentage of neoformed osteoid matrix (%OM). In both groups studied, at all biological points, deposition of reparative osteoid matrix (OM) was observed near the bone edges; discrete chronic inflammatory response; connective tissue formation and neovascularization in the residual area of the defect. In the GnHASr, in the two evaluated periods, the deposition of OM was also noticed, both around and inside the microspheres. At 60 days, an area of 7.54% of OM deposition in relation to the total defect area was evidenced in the GnHASr, while in the CG this value was 6.80%. It is concluded that the nHASr microspheres evaluated were biocompatible, biodegradable, bioresorbable, bioactive and osteoconductive. In both groups, the formation of neomineralized tissue occurred in a limited way, which indicates that the concentration of metal used in the replacement did not favor greater osteogenic potential for the biomaterial. The evaluated biomaterial it's adequate for use as a filling material.

Keywords: Biomaterials; Bone regeneration; Critical bone defect; Hydroxyapatite; Strontium.

Resumo

O objetivo deste estudo foi analisar o comportamento biológico e potencial osteogênico de microesferas de hidroxiapatita nanoestruturadas substituídas com estrôncio (nHASr). Para tanto, utilizou-se vinte ratos wistar, adultos, machos, distribuídos, aleatoriamente, em dois grupos: GnHASr – defeito ósseo crítico preenchido com microesferas de nHASr; e GC (grupo controle) – defeito ósseo crítico sem implantação de biomaterial; avaliados nos pontos biológicos

de 30 e 60 dias. Os espécimes foram processados e corados por hematoxilina-eosina (HE) e tricrômico de Masson-Goldner (TG), e examinados por microscopia de luz comum. Posteriormente, foram analisados histomorfometricamente, para mensuração do percentual de matriz osteoide neoformada (%MO). Nos dois grupos estudados, em todos os pontos biológicos, observou-se deposição de matriz osteoide (MO) reparativa, próxima às bordas ósseas; resposta inflamatória crônica discreta; formação de tecido conjuntivo e neovascularização na área residual do defeito. No GnHASr, nos dois períodos avaliados, a deposição de MO foi notada, também, tanto de forma circunjacente quanto no interior das microesferas. Aos 60 dias, evidenciou-se no GnHASr uma área de 7,54% de deposição de MO em relação a área total do defeito, enquanto no GC este valor foi de 6,80%. Conclui-se que as microesferas de nHASr avaliadas neste estudo foram biocompatíveis, biodegradáveis, biorreabsorvíveis, bioativas e osteocondutoras. Nos dois grupos, a formação de tecido neomineralizado ocorreu de forma limitada, isto indica que a concentração de metal utilizada na substituição não favoreceu maior potencial osteogênico ao biomaterial. O biomaterial avaliado é adequado para ser utilizado como material de preenchimento.

Palavras-chave: Biomateriais; Regeneração óssea; Defeito ósseo crítico; Hidroxiapatita; Rato; Estrôncio.

Resumen

El objetivo de este estudio fue analizar el comportamiento biológico y el potencial osteogénico de microesferas de hidroxiapatita nanoestructuradas sustituidas con estrôncio (nHASr). Para tanto, veinte ratas wistar macho adultas se distribuyeron aleatoriamente en dos grupos: GnHASr – defecto óseo crítico relleno con microesferas nHASr; e GC (grupo de control) - defecto óseo crítico sin implantación de biomaterial; evaluado en los puntos biológicos de 30 y 60 días. Los especímenes recolectados fueron processados y teñidos con hematoxilina-eosina (HE) y tricrômico de Masson-Goldner (TG), y examinados por microscopía de luz común. Posteriormente, se analizaron histomorfométricamente para medir el porcentaje de matriz osteoide neoformada (%MO). En ambos grupos estudiados, en todos los puntos biológicos se observó depósito de matriz osteoide (MO) reparadora, cerca de los bordes óseos; respuesta inflamatoria crónica leve; formación de tejido conectivo y neovascularización en el área residual del defecto. En el GnHASr, en los dos periodos evaluados, también se notó la deposición de MO, tanto alrededor como dentro de las microesferas. A los 60 días se evidenció en el GnHASr un área de 7,54% de depósito de MO con relación al área total del defecto, mientras que en el GC este valor fue de 6,80%. Se concluye que las microesferas de nHASr evaluadas en este estudio fueron biocompatibles, biodegradables, biorreabsorbibles, bioactivas y osteocondutoras. En ambos grupos, la formación de tejido neomineralizado ocurrió de forma limitada, lo que indica que la concentración de metal utilizada en el reemplazo no favoreció un mayor potencial osteogénico para el biomaterial. El biomaterial evaluado es adecuado para su uso como material de relleno.

Palabras clave: Biomateriales; Regeneración ósea; Defecto óseo crítico; Hidroxiapatita; Estroncio.

1. Introduction

Extensive bone lesions resulting from trauma, osteotomies, tumor resections, and automobile accidents, among others, may compromise the functionality and aesthetics of the affected area since, in these losses, the bone repair is completed by fibrosis (Porto et al., 2012; Spicer et al., 2012; Miguel et al., 2013; Santos et al., 2019; Santos et al., 2021a; Santos et al., 2021b). These situations characterize an excellent challenge for health professionals and researchers in Bone Tissue Bioengineering, who have researched and improved and, when possible, clinically used different regenerative techniques and biomaterials to stimulate tissue regeneration in these inhospitable conditions.

Among the synthetic biomaterials most used in these situations, calcium phosphates, especially hydroxyapatite (HA) and tricalcium phosphate (TCP), which have been widely investigated, mainly due to bioactivity, absence of toxicity and similarity with the mineral phase of bone tissue, as well as the biocompatibility that these materials present (Shepherd et al., 2012; Valiense et al., 2015; Machado et al., 2016; Carmo et al., 2018; Winkler et al., 2018). Nevertheless, the biodegradation rate of these biomaterials depends on the techniques used during the synthesis and processing of these ceramics (Carmo et al., 2018).

The development of biomimetic materials, such as nanostructured HA (nHA), has gained scientific notoriety due to its promising clinical application since it promotes changes in the physical-chemical properties of the material that may reflect better results after in vivo implantation. The reduction of particle size promotes an increase in the surface area, which consequently decreases crystallinity, increases the biodegradability and bioactivity of ceramics, and approximates biological

apatite (Cai et al., 2007; Shepherd et al., 2012; Mir et al., 2012; Carmo et al., 2018; Cuzzo et al., 2020).

During the synthesis of these biomaterials, the calcium substitution (Ca) in the structure of HA by metals present in bone tissue, such as fluoride (F), strontium (Sr), magnesium (Mg), and zinc (Zn), has also attracted scientific and clinical interest, since these modifications promote changes in the physical-chemical properties of ceramics and, consequently, alterations in biological response (Calasans-Maia et al., 2014; Liu et al., 2019; Harrison et al., 2021; Santos et al., 2021b). Among these, Sr ion is highlighted, which stimulates the differentiation and proliferation of osteoblasts with consequent bone matrix formation, as well as promotes the reduction of differentiation and activity of osteoclasts, which provides increased bone mineral density (BMD) (Ammann et al., 2004; Bonnelye et al., 2008; Querido et al., 2016; Marx et al., 2020; Kołodziejaska et al., 2021; Borciani et al., 2022). According to Bootchanont et al. (2017), the Sr replacement in the structure of HA modifies its thermal stability, solubility, texture, and surface reactivity. Furthermore, it alters the biomaterial's porosity and favors osteoblasts' adhesion, proliferation, and differentiation with consequent osteoid matrix neof ormation (Shepherd et al., 2012; Valiense et al., 2015).

This dual role has instigated the development of new studies that support the understanding of the influence of this metal on bone repair, especially in association with HA (Ehret et al., 2017; Carmo et al., 2018; Luo et al., 2018; Má et al., 2021; Jiang et al., 2022; Liu et al., 2023). Given the above, this study aims to analyze the biological behavior and osteogenic potential of nanostructured hydroxyapatite microspheres replaced with Sr (nHASr) after implantation in a critical bone defect in adult rat calvaria.

2. Methodology

2.1 Biomaterials

The biomaterials evaluated in this study were synthesized, processed, characterized, and transferred by researchers from the Biomaterials Laboratory (LABIOMAT) at the Brazilian Center for Physics Research (CBPF), in Rio de Janeiro (RJ), Brazil.

2.1.1 Synthesis and processing of nHASr microspheres

For the synthesis of biomaterial, solutions of Ca nitrate (*Merck*[®], Darmstadt, Hessen, Germany), Sr nitrate (*Merck*[®], Darmstadt, Hessen, Germany), and ammonium hydroxide (*Merck*[®], Darmstadt, Hessen, Germany) were used. Hydroxyapatite was primarily synthesized as a nanometric powder with crystals of dimensions lower than 10 nm through wet precipitation routes. The powder obtained was submitted to a deagglomeration process by treatment with high-power ultrasound and deagglomerating material with controlled pH conditions. Subsequently, Sr was added, using Sr nitrate, at a concentration of 1%. Then, the nHASr powder was mixed with a sodium alginate solution (*Sigma-Aldrich*[®], Saint Louis, Missouri, United States) in a ratio of 15:1, under slight agitation, until obtaining a homogeneous paste. Once this was done, this paste was dripped in a dihydrated calcium chloride solution (*Merck*[®], Darmstadt, Hessen, Germany) to immediately form the microspheres, which remained in this solution for 24 hours for complete gelling. After this period, the biomaterial was washed in ultrapure water (Milli-Q[®], Millipore Corp.), lyophilized, and dried in an oven at 60°C for 24 hours. The microspheres were separated according to the granulometric range of 425 to 600 µm, packed in an *Eppendorf microtube*, and sterilized with gamma rays.

2.1.2 Physicochemical characterization of nHASr microspheres

2.1.2.1 Surface Area

The surface area obtained by the BET method (ASAP 2020, *Micromeritics Instrument Corporation*[®], Norcross, Georgia, USA) was 75.38 m²/g different from the area of a HA - 35.95m²/g (Scudeller et al., 2017).

2.1.2.2 Chemical Composition

The chemical composition and stoichiometry of the microspheres were determined by the Atomic Absorption Spectrometry (AAS) technique (Shimadzu AA 6800, *Shimadzu Corporation*[®], Chiyoda, Tokyo, Japan)(Table 1).

Table 1 - Atomic Absorption Spectrometry (AAS) technique of nHASr and HA stoichiometric microspheres.

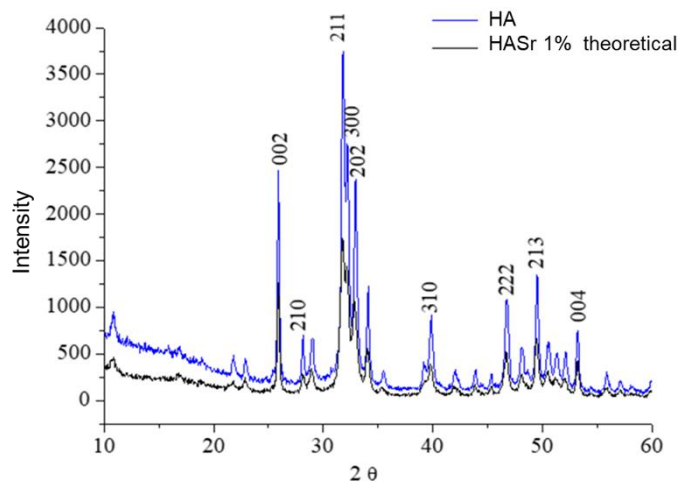
Sample	Ca %	Ca mol	P %	P mol	Sr %	Sr mol	Ca/P Ratio
HA	36.28	0.905	16.73	0.540	-	-	1.675
nHASr	43.80	1.093	17.50	0.565	0.43	0.005	1.935

Source: Brazilian Center for Physics Research (CBPF).

2.1.2.3 X-Ray Diffraction (XRD)

The crystallinity of the microspheres was obtained by the RX diffraction technique, using a high-resolution diffractometer system (HZG4, *Zeiss*[®], Jena, Thuringia, Germany) operating at 30kV and 15mA with Cu K α radiation ($\lambda=1.542\text{\AA}$)(Figure 1). The nHASr microspheres presented the basis of the prominent peaks wider than those observed in HA, which evidences a lower crystallinity of the biomaterial containing Sr.

Figure 1 - XRD of nSrHA and HA.

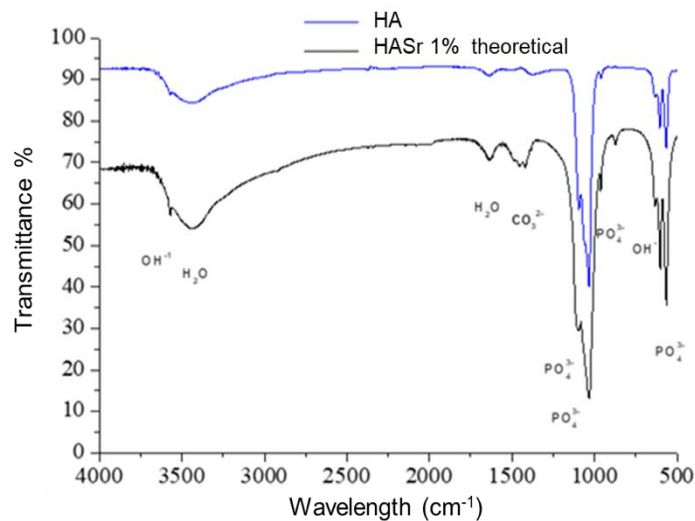


It is noted that the base of the prominent peaks of nSrHA is slightly wider than the base of the HA peaks, demonstrating a lower crystallinity of HA with the Sr ion. Source: Brazilian Center for Physics Research (CBPF).

2.1.2.4 Fourier Transform Infrared Spectroscopy (FTIR)

Fourier Transform Infrared Spectroscopy (FTIR –IR, Prestige 21 spectrometer Shimadzu, *Shimadzu Corporation*[®], Chiyoda, Tokyo, Japan) revealed typical bands of a HA for phosphate (PO_4^{3-}), water (H_2O), and hydroxyl (OH^{1-}). In nHASr, the presence of carbonate in the 1438 cm^{-1} bands was also noted, indicating alginate's presence. The presence of extensive and intense water bands proves that the microspheres were not heat-treated (Figure 2).

Figure 2 - FTIR of nHASr and HA.



The presence of typical bands of a HA for phosphate (PO_4^{3-}), water (H_2O), and hydroxyl (OH^-) is observed. Source: Brazilian Center for Physics Research (CBPF).

2.2 Experimental procedures

2.2.1 Animals

After approval by the Ethics Committee on the Use of Animals (CEUA) of the Institute of Health Science (ICS) of the Federal University of Bahia (UFBA), protocol no. 063/2014, twenty male adult *Wistar* rats weighing between 350 and 400g and three to four months of age were randomly divided into two experimental groups: GnHASr – critical bone defect filled with nHASr microspheres; and CG - critical bone defect without implantation of biomaterials (control group). These animals were evaluated, with five animals in each group/period, at 30 and 60 days postoperative biological points. Throughout the experimental period, the animals were kept separated in propylene boxes, identified according to the experimental group and biological point; and fed with a standard solid diet and water *ad libitum*.

2.2.2 Surgical procedures

After general anesthesia (0.1mL/100g ketamine hydrochloride) and analgesia (xylazine hydrochloride 0.04mL/100g), trichotomy and antisepsis with 1% chlorhexidine were performed in the calvarial region. Then, the circular critical bone defect was made in the median part of the calvaria, approximately 8.5 mm in diameter. Once this was done, the biomaterial was implanted, except in the animals of the control group, and the skin flap was repositioned and sutured with simple stitches, as described by Miguel et al. (2006) and illustrated by Santos et al. (2019).

2.2.3 Laboratory Stage and Histomorphometric Analysis

At the biological points of 30 and 60 days, the animals were euthanized with a lethal dose of anesthetic to remove the upper part of the calvaria discarding the surrounding soft tissues. Then, the specimens were fixed in 4% buffered formaldehyde for 72h. Subsequently, the samples were decalcified in 5% EDTA for seven days and included in paraffin. The specimens were cut in the transverse direction of the calvaria with five μm thickness, stained by hematoxylin-eosin (HE) and Masson-Goldner trichrome stain (TG), and examined by common light microscopy (Microscope DM6M, *Leica*[®], Nußloch, Baden-Württemberg,

Germany). The photomicrographs were obtained using the Digital Camera DFC310FX (*Leica*[®], Wetzlar, Germany) coupled to the Optical Microscope DM6 B (*Leica*[®], Wetzlar, Germany). For histomorphometric analysis, LAS - *Leica Application Suite* software (*Leica*[®], Nußloch, Baden-Württemberg, Germany) was used to measure the percentage of the neoformed osteoid matrix (%OM) concerning the total area of the defect. The values obtained were described by mean and standard deviation and evaluated by the *Wilcoxon Signed Ranks Test*.

3. Results

3.1 Histological analysis

At the biological point of 30 days, in both experimental groups, bone neoformation was noted restricted to the edges of the defect, with the presence of osteocytes (Figures 3A and B). At 60 days, in the GnHASr, this finding extended, in the centripetal direction to the defect, adjacently and permeated the particles of the biomaterial and was more organized than in the previous period, with the formation of concentric lamellae (Figure 4A and C). At this biological point, in the CG, bone neoformation remained restricted to the edges but without lamella formation (Figure 4B and D). In both groups, in both biological points, the residual area of the defect was filled by connective tissue with reduced thickness concerning the bone border (Figure 3E and F) (Figure 4E and F). In GnHASr, this tissue was rich in blood vessels (Figure 3E)(Figure 4E). Nevertheless, in the CG, this tissue presented a fibrous and slender aspect (Figure 3F)(Figure 4F).

In the GnHASr, throughout the experimental period, the biomaterial was now intact or fragmented (Figure 3A, C, and E)(Figure 4A, C, and E). In the regions near the bone edges, the microspheres were surrounded and permeated by bone neoformation and loose connective tissue (Figure 3A and C)(Figure 4A and C). In both groups, in the two biological points, mild chronic inflammation was observed with mononuclear inflammatory infiltrate (Figure 3E and F)(Figure 4E and F). In GnHASr, this response was of the chronic granulomatous type, with few multinucleated giant cells surrounding the biomaterial particles (Figure 3E)(Figure 4A and E).

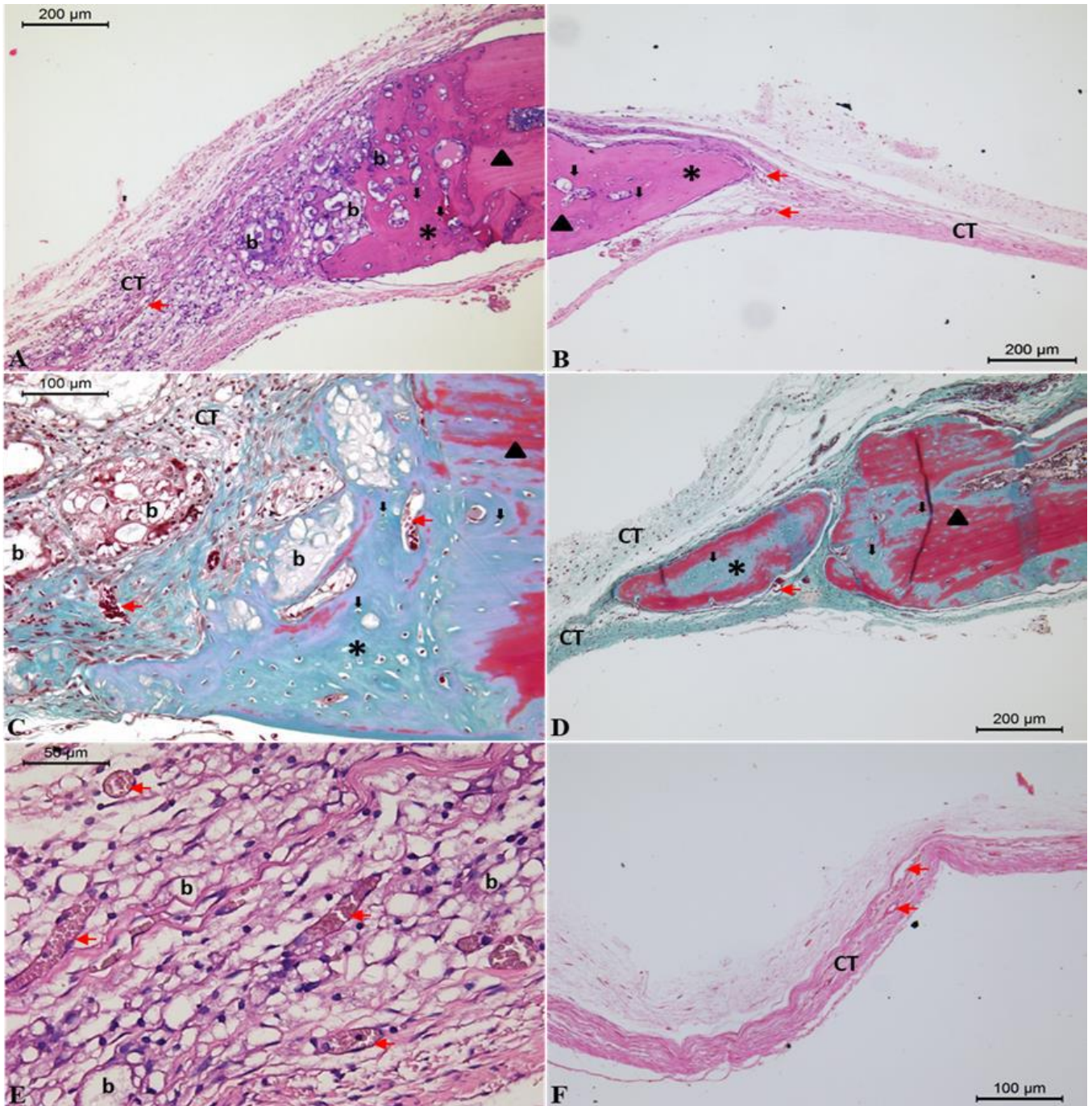
3.2 Histomorphometric analysis

The histomorphometric analysis of the mineralized area concerning the total area of the defect showed that this tissue was observed in both groups throughout the experiment. However, the non-parametric *Wilcoxon signed rank test* comparison between the means obtained in the groups showed no statistically significant difference in any of the studied biological points ($p = 0.686$) (Figure 5).

4. Discussion

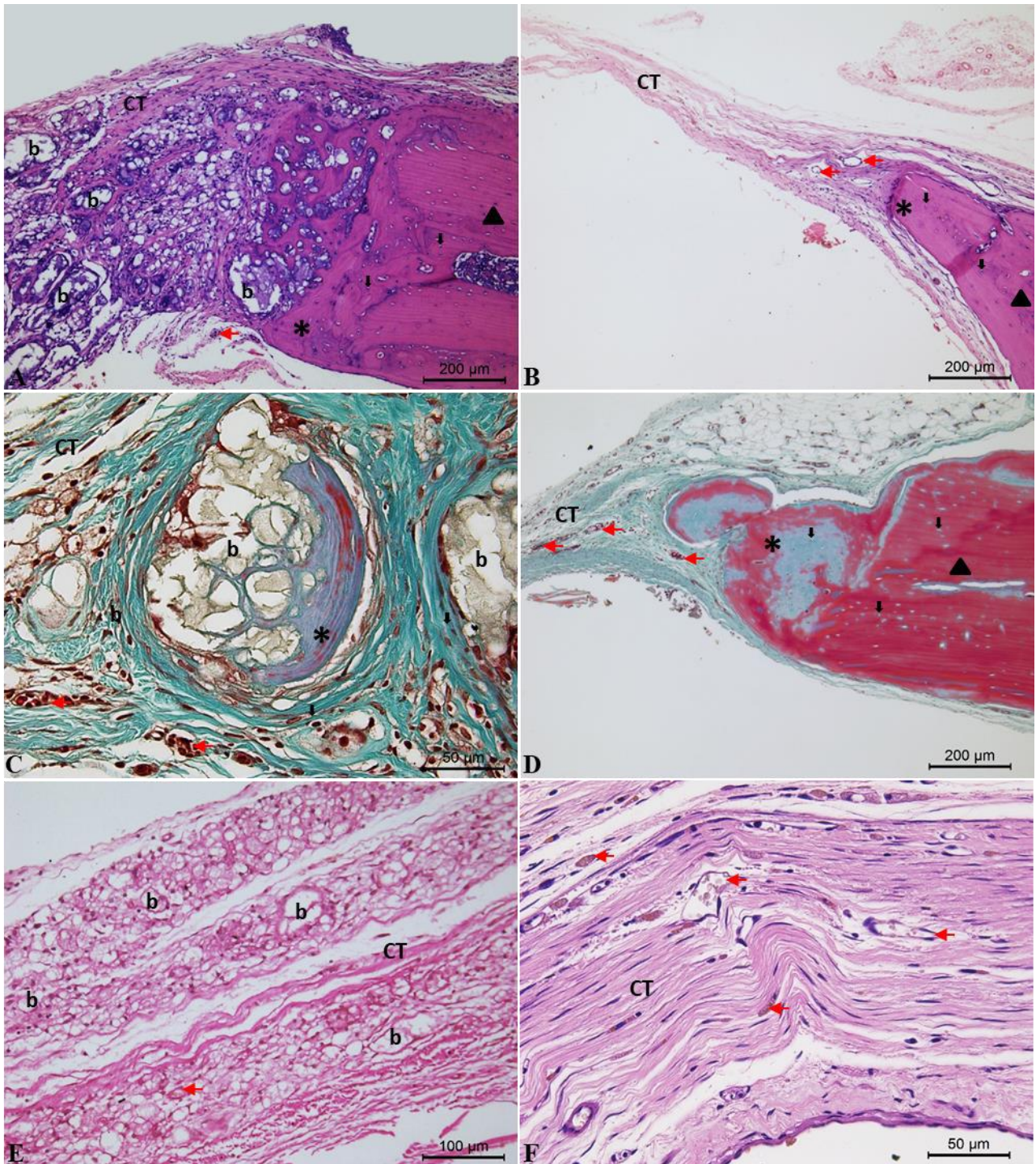
Critical bone defects have been an experimental model widely used in vivo studies involving the evaluation of the mechanism of bone regeneration because this site has anatomical and physiological characteristics that allow easy access, reproducibility, and surgical manipulation; does not require postoperative fixation; and has a reduced risk of post-surgical complications (Spicer et al., 2012). Furthermore, the bone defect produced has critical morphological characteristics of extension and width, in which spontaneous bone regeneration does not occur throughout the animal life, which makes it possible to ascertain the osteogenic potential of the biomaterial (Schmitz & Hollinger, 1986). The histological findings of the CG demonstrated these characteristics throughout this study since bone neoformation remained restricted to the edges of the defect, with the formation of fibrous connective tissue in the remaining area (Miguel et al., 2006; Miguel et al., 2013; Ribeiro et al., 2015; Santos et al., 2019; Almeida et al., 2020; Santos et al., 2021b).

Figure 3 - Photomicrographs of GnHASr and CG at the 30-day biological point.



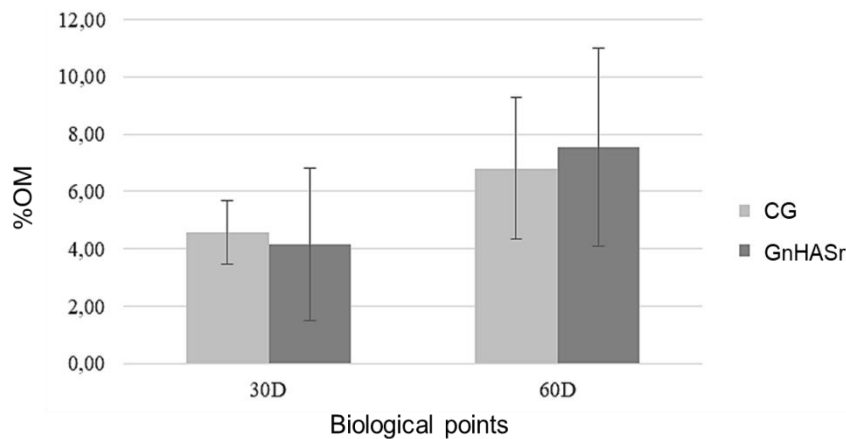
Note neoformed osteoid matrix (asterisk), with the presence of osteocytes (black arrow) adjacent to the edge of the bone defect (black triangle) and surrounding the biomaterial (b) (GnHASr); the presence of blood vessels (red arrow) in the connective tissue (CT). (A) GnHASr - HE; (B) GC - HE; (C) GnHASr - TG; (D) CG - TG; (E) GnHASr - HE; (F) CG - HE. Source: Elaborated by the authors.

Figure 4 - Photomicrographs of GnHASr and CG at the 60-day biological point.



Note neoformed osteoid matrix (asterisk), with the presence of osteocytes (black arrow); blood vessels (red arrow) in connective tissue (CT); particles of the biomaterial (b) near the margin of the bone defect (black triangle) integrated into the remaining bone tissue through the neoformed osteoid matrix that is sometimes shown to be the presence of concentric lamellae (asterisk). (A) GnHASr - HE; (B) CG - HE; (C) GnHASr - TG; (D) CG - TG; (E) GnHASr - HE; (F) CG - HE. Elaborated by the authors.

Figure 5 -Percentage of the neoformed osteoid matrix (%OM) at biological points of 30 and 60 days in both groups - GnHASr and CG.



Source: Elaborated by the authors.

In the GnHASr, the interstice formed between the microspheres enabled angiogenesis; the diffusion of nutrients and growth factors; migration, cell proliferation, and differentiation, particularly of the osteoblastic lineage; and, thus, the formation of a new bone matrix in addition to the percentage observed in the CG (Petrovic et al., 2012; Valiense et al., 2015; Costa et al., 2016; Carmo et al., 2018; Buchaim et al., 2022). This occurred due to the 3D framework provided by the biomaterial, which was biocompatible, biodegradable, and osteoconductive, essential characteristics of bone neoformation. On the other hand, in CG, the absence of a scaffold culminated in a lower bone neoformation percentage and was strictly limited to the edges. In both groups, the residual area had the repair completed by the formation of connective scar tissue, as evidenced in other studies (Cardoso et al., 2006; Miguel et al., 2006; Miguel et al., 2013; Ribeiro et al., 2015; Santos et al., 2019; Almeida et al., 2020; Santos et al., 2021b).

In the case of experimental studies, the surgical procedure used to make the critical bone defect, and extensive bone loss, under clinical conditions, causes vascular ruptures due to tissue lesions. These promote the release of cytokines and chemical mediators that initiate an inflammatory response in parallel to the formation of the blood clot (Anderson et al., 2008), which was evidenced in the results of the two groups evaluated in this study and is in agreement with what was observed by Cardoso et al., 2006, Miguel et al., 2006, Almeida et al., 2015, Ribeiro et al., 2015, Valiense et al., 2015, Carmo et al., 2018; Santos et al., 2019, Santos et al., 2021a and Santos et al., 2021b. In histological findings, the inflammatory response observed was of the chronic, discrete, and regressive type throughout the study, which, according to Anderson et al. (2008), is expected after the implantation of biomaterials (Cardoso et al., 2006; Miguel et al., 2006; Almeida et al., 2015; Ribeiro et al., 2015; Valiense et al., 2015; Carmo et al., 2018; Santos et al., 2021a; Santos et al., 2021b). The intensity and duration of the inflammatory response prove the biomaterial's biocompatibility, consequently guiding the clinical application of this.

Biological HA is a carbonated, non-stoichiometric apatite with some ions in its structure, such as F, Mg, Zn, and Sr (Li et al., 2012; Yatongchai et al., 2015; Combes et al., 2016; Machado et al., 2016). Thus, performing ionic substitutions, with specific ions, in the structure of synthetic HA can bring it closer to the biological one; modify its crystallinity and solubility; and directly interfere with its biodegradability, relevant characteristics in bone regeneration (Combes et al., 2016; Ratnayake et al., 2016; Tite et al., 2018; Harrison et al., 2021; Ma et al., 2021). In the present study, substituting part of the Ca ions of nHA by Sr – 1% theoretical guaranteed a practical percentage of 0.43% of Sr. This value provided slight changes in the physical-

chemical properties of the microspheres – the lower crystalline, evidenced by the XRD (Figure 4), which probably influenced the fragmentation of the biomaterial, since the lower the crystalline, the greater the solubility of HA (Machado et al., 2010; Conz et al., 2011; Kammer et al., 2016; Carmo et al., 2018).

It is known that Sr acts positively on bone neoformation, stimulating the differentiation and proliferation of osteoblasts, and negatively on bone reabsorption by inhibiting the action of osteoclasts (Querido et al., 2016; Carmo et al., 2018; Marx et al., 2020; Harrison et al., 2021; Kołodziejska et al., 2021; Ma et al., 2021; Borciani et al., 2022; You et al., 2022). In this study, the partial replacement of Sr in the structure of HA favored a higher percentage of bone neoformation in the GnHASr. However, the values observed were not statistically significant concerning the CG. These findings corroborate the results found by Luo et al. (2018), who evaluated a framework of HA replaced with Sr in a critical defect in rabbit calvaria and, similarly to our study, found greater bone neoformation in the group with metal presence. However, these authors used the Sr in the concentration of 5% theoretical and 1.61% practical. Machado et al. (2016), when using HA microspheres replaced with 1% Sr, observed the lowest percentage of bone neoformation in the metal group, different from our results. It is note point that these authors used ewe as an experimental model and implanted the biomaterials in a different anatomical site – ewe tibias.

In line with the biomimetic principles, during the development of the biomaterial, one can also opt for the synthesis of nanostructured materials, which are more similar to biological HA, given the size of the crystals, less than 100 nm; better biocompatibility; and reabsorption of particles of the material more quickly and homogeneously (Su et al., 2003; Lala et al., 2014; Wang et al., 2014; Valiense et al., 2015). Moreover, these materials show a larger surface area concerning conventional materials, which favors the migration, fixation, differentiation, and proliferation of cells surrounding the biomaterial. They may thus justify the biodegradation observed in the GnHASr microspheres evaluated in this study and the formation of the osteoid matrix surrounding the biomaterial (Valenzuela et al., 2012; Aina et al., 2013).

Given the biocompatibility presented by the biomaterial evaluated in this study, further research using a higher theoretical concentration of Sr should be developed to identify which concentration is appropriate for a more evident bone neoformation.

5. Conclusion

The nHASr microspheres evaluated in this study were biocompatible, biodegradable, bioresorbable, bioactive, and osteoconductive, making them promising for future clinical use. The formation of neomineralized tissue was limited in both groups. This indicates that the Sr concentration used in the substitution did not favor a more significant osteogenic potential to the biomaterial. Therefore, new studies need to be developed in order to identify concentrations of this metal that may contribute to new bone formation, in view of its important role in this tissue.

Acknowledgments

The authors appreciate the financial support of the National Council for Scientific and Technological Development (CNPq)[SUS0010/2013] and the Foundation for Research Support of the State of Bahia (FAPESB) through granting of the scholarship.

References

Aina, V., Bergandi, L., Lusvardi, G., Malavasi, G., Imrie, F. E., Gibson, I. R., Cerrato, G. & Ghigod, D. (2013). Sr-containing hydroxyapatite: morphologies of HA crystals and bioactivity on osteoblast cells. *Materials Science and Engineering: C*, 33(3), 1132-1142.

- Ammann, P., Shen, V., Robin, B., Mauras, Y., Bonjour, J. & Rizzoli, R. (2004). Strontium Ranelate Improves Bone Resistance by Increasing Bone Mass and Improving Architecture in Intact Female Rats. *Journal of Bone and Mineral Research*, 19(12), 2012-2020.
- Anderson, J. M., Rodriguez, A. & Chang, D. T. (2008). Foreign body reaction to biomaterials. *Seminars in Immunology*, 20(2), 86-100.
- Bonnelye, E., Chabadel, A., Saltel, F. & Jurdic, P. (2008). Dual effect of strontium ranelate: Stimulation of osteoblast differentiation and inhibition of osteoclast formation and resorption in vitro. *Bone*, 42(1), 129-138.
- Bootchanont, A., Sailuam, W., Sutikulsoat, S., Temprom, L., Chanlek, N., Kidkhunthod, P., Suwanna, P. & Yimmirun, R. (2017). Synchrotron X-ray Absorption Spectroscopy study of local structure in strontium-doped hydroxyapatite. *Ceramics International*, 43(14), 11023-11027.
- Borciani, G., Ciapetti, G., Vitale-Brovarone, C. & Baldini, N. (2022). Strontium Functionalization of Biomaterials for Bone Tissue Engineering Purposes: A Biological Point of View. *Materials*, 15, 1724.
- Buchaim, D. V., Andreo, J. C., Pomini, K. T., Barraviera, B., Ferreira Júnior, R. S., Duarte, M. A. H., Alcalde, M. P., Reis, C. H. B., Teixeira, D. B., Bueno, C. R. S., Detregiachi, C. R. P., Araujo, A. C. & Buchaim, R. L. (2022). A biocomplex to repair experimental critical size defects associated with photobiomodulation therapy. *Journal of Venomous Animals and Toxins including Tropical Diseases*, 28, e20210056.
- Cai, Y., Liu, Y., Yan, W., Hu, Q., Tao, J., Zhang, M., Shi, Z. & Tang, R. (2007). Role of hydroxyapatite nanoparticle size in bone cell proliferation. *Journal of Materials Chemistry*, 17, 3780-3787.
- Calasans-Maia, M., Calasans-Maia, J., Santos, S., Mavropoulos, E., Farina, M., Lima, I., Lopes, R. T., Rossi, A. & Granjeiro, J. M. (2014). Short-term in vivo evaluation of zinc-containing calcium phosphate using a normalized procedure. *Materials Science and Engineering: C*, 41, 309-319.
- Carmo, A. B. X., Sartoretto, S. C., Alves, A. T. N. N., Granjeiro, J. M., Miguel, F. B., Calasans-Maia, J. & Calasans-Maia, M. D. (2018). Alveolar bone repair with strontium-containing nanostructured carbonated hydroxyapatite. *Journal of Applied Oral Science*, 26, e20170084.
- Combes, C., Cazalbou, S. & Rey, C. (2016). Apatite Biominerals. *Minerals*, 6(2), 1-25.
- Conz, M. B., Granjeiro, J. M. & Soares, G. A. (2011). Hydroxyapatite crystallinity does not affect the repair of critical size bone defects. *Journal of Applied Oral Science*, 19(4), 337-42.
- Costa, N. M., Yassuda, D. H., Sader, M. S., Fernandes, G. V., Soares, G. D., & Granjeiro, J. M. (2016). Osteogenic effect of tricalcium phosphate substituted by magnesium associated with Genderm[®] membrane in rat calvarial defect model. *Materials Science and Engineering C*, 61(1), 63-71.
- Cuozzo, R. C., Sartoretto, S. C., Resende, R. F. B., Alves, A. T. N. N., Mavropoulos, E., Prado da Silva, M. H. & Calasans-Maia, M. D. (2020). Biological evaluation of zinc-containing calcium alginate-hydroxyapatite composite microspheres for bone regeneration. *Journal of Biomedical Materials Research Part B: Applied Biomaterials*, 1-11.
- Ehret, C., Aid-Launais, R., Sagardoy, T., Siadous, R., Bareille, R., Rey, S., Pechev, S., Etienne, L., Kalisky, J., Mones, E., Letourneur, D., & Amedee Vilamitjana, J. (2017). Strontium-doped hydroxyapatite polysaccharide materials effect on ectopic bone formation. *PLOS ONE*, 12(9), 1-21.
- Harrison, C. J., Hatton, P. V., Gentile, P. & Miller, C. A. (2021). Nanoscale Strontium-Substituted Hydroxyapatite Pastes and Gels for Bone Tissue Regeneration. *Nanomaterials*, 11(6), 1611.
- Jiang, S., Wang, X., Ma, Y., Zhou, Y., Liu, L., Yu, F., Fang, B., Lin, K., Xia, L. & Cai, M. (2022). Synergistic Effect of Micro-Nano-Hybrid Surfaces and Sr Doping on the Osteogenic and Angiogenic Capacity of Hydroxyapatite Bioceramics Scaffolds. *International Journal Nanomedicine*, 17, 783-797.
- Kammer, G. M., Sartoretto, S. C., Resende, R., Uzeda, M., Nascimento, J. R., Alves, A. T., Calasans-Maia, J., Rossi, A. M., Granjeiro, J. M. & Calasans-Maia, M. D. (2016). In vivo evaluation of strontium-containing nanostructured carbonated hydroxyapatite. *Key Engineering Materials*, 696, 212-222.
- Kołodziejaska, B., Stepien, N. & Kolmas, J. (2021). The Influence of Strontium on Bone Tissue Metabolism and Its Application in Osteoporosis Treatment. *International Journal of Molecular Sciences*, 22, 6564.
- Lala, S., Brahmachari, S., Das, P. K., Das, D., Kar, T. & Pradhan, S. K. (2014). Biocompatible nanocrystalline natural bonelike carbonated hydroxyapatite synthesized by mechanical alloying in a record minimum time. *Materials Science and Engineering C*, 42, 647-656.
- Li, B., Liao, X., Zheng, L., He, H., Wang, H., Fan, H. & Zhang, X. (2012). Preparation and cellular response of porous A-type carbonated hydroxyapatite nanoceramics. *Materials Science and Engineering C*, 32, 929-936.
- Liu, S., Zhou, H., Liu, H., Ji, H., Fei, W. & Luo, E. (2019). Fluorine-contained hydroxyapatite suppresses bone resorption through inhibiting osteoclasts differentiation and function in vitro and in vivo. *Cell Proliferation*, 52(3), e12613.
- Liu, X., Huang, H., Zhang, J., Sun, T., Zhang, W. & Li, Z. (2023). Recent Advance of Strontium Functionalized in Biomaterials for Bone Regeneration. *Bioengineering*, 10, 414.
- Luo, Y., Chen, S., Shi, Y. & Ma, J. (2018). 3D printing of strontium-doped hydroxyapatite based composite scaffolds for repairing critical-sized rabbit calvarial defects. *Biomedical Materials*, 13(6), 065004.
- Ma, P., Chen, T., Wu, X., Hu, Y., Huang, K., Wang, Y. & Dai, H. (2021). Effects of bioactive strontium-substituted hydroxyapatite on osseointegration of polyethylene terephthalate artificial ligaments. *Journal of Materials Chemistry B*, 9, 6600-6613.
- Machado, C. P. G., Pintor, A. V. B., Gress, M. A. K. A., Rossi, A. M., Granjeiro, J. M & Calasans Maia, M. D. (2010). Avaliação da hidroxiapatita contendo estrôncio como substituto ósseo em tíbias de ovelhas. *Innovations Implant Journal: Biomaterials and Esthetics*, 5(1), 9-14.

- Machado, C. P. G., Sartoretto, S. C., Alves, A. T. N. N., Lima, I. B. C., Rossi, A. M., Granjeiro, J. M. & Calasans-Maia, M. D. (2016). Histomorphometric evaluation of strontium-containing nanostructured hydroxyapatite as bone substitute in sheep. *Brazilian Oral Research*, 30(1), e45 1-11.
- Marx, D., Rahimnejad Yazdi, A., Papini, M. & Towler, M. (2020). A review of the latest insights into the mechanism of action of strontium in bone. *Bone Reports*, 12, 100273.
- Miguel, F. B., Barbosa Júnior, A. A., de Paula, F. L., Barreto, I. C., Goissis, G. & Rosa, F. P. (2013). Regeneration of critical bone defects with anionic collagen matrix as scaffolds. *Journal of Materials Science: Materials in Medicine*, 24(11), 2567-2575.
- Miguel, F.B., Cardoso, A. K. M. V., Barbosa Júnior, A. A., Marcantonio Júnior, E., Goissis, G. & Rosa, F. P. (2006). Morphological assessment of the behavior of three-dimensional anionic collagen matrices in bone regeneration in rats. *Journal of Biomedical Materials Research Part B: Applied Biomaterials*, 78B(2), 334-339.
- Mir, M., Leite, F. L., Herrmann Junior, P. S. P., Pissetti, F. L., Rossi, A. M., Moreira, E. L. & Mascarenhas, Y. P. (2012). XRD, AFM, IR and TGA Study of Nanostructured Hydroxyapatite. *Materials Research*, 15(4), 622-627.
- Petrovic, M., Colovic, B., Jokanovic, V. & Markovic, D. (2012). Self assembly of biomimetic hydroxyapatite on the surface of different polymer thin films. *Journal of Ceramic Processing Research*, 13(4), 398-404.
- Porto, G. G., Vasconcelos, B. C. E., Andrade, E. S. S., Carneiro, S. C. A. S. & Frota, M. S. M. (2012). Is a 5 mm rat calvarium defect really critical? *Acta Cirurgica Brasileira*, 27(11), 757-760.
- Querido, W., Rossi, A. L. & Farina, M. (2016). The effects of strontium on bone mineral: A review on current knowledge and microanalytical approaches. *Micron*, 80, 122-134.
- Ratnayake, J. T. B., Mucalo, M. & Dias, G. J. (2016). Substituted hydroxyapatites for bone regeneration: a review of current trends. *Journal of Biomedical Materials Research Part B: Applied Biomaterials*, 105, 1285-99.
- Ribeiro, I. I. A., Almeida, R. S., Rocha, D. N., Prado da Silva, M., Miguel, F. B. & Rosa, F. P. (2015) Biocerâmicas e polímero para a regeneração de defeitos ósseos críticos. *Revista de Ciências Médicas e Biológicas*, 13(3), 298-302.
- Santos, G. G., Miguel, I. R. J. B., Barbosa Junior, A. A., Barbosa, W. T., Almeida, K. V., García-Carrodegua, R., Fook, M. L., Rodríguez, M. A., Miguel, F. B., Araújo, R. P. C. & Rosa, F. P. (2021a). Bone regeneration using Wollastonite/ β -TCP scaffolds implants in critical bone defect in rat calvaria. *Biomedical Physics & Engineering Express*, 7, 055015, 1-17.
- Santos, G. G., Nunes, V. L. C., Marinho, S. M. O. C., Santos, S. R. A., Rossi, A. M. & Miguel, F. B. (2021b). Biological behavior of magnesium-substituted hydroxyapatite during bone repair. *Brazilian Journal of Biology*, 81(1), 53-61.
- Santos, G. G., Vasconcelos, L. Q., Poy, S. C. S., Almeida, R. S., Barbosa Júnior, A. A., Santos, S. R. A., Rossi, A. M., Miguel, F. B. & Rosa, F. P. (2019). Influence of the geometry of nanostructured hydroxyapatite and alginate composites in the initial phase of bone repair. *Acta Cirúrgica Brasileira*, 34(2), e201900203
- Schmitz, J. P. & Hollinger, J. O. (1986). The critical size defect as an experimental model for craniomandibulofacial nonunions. *Clinical Orthopaedics and Related Research*, (205), 299-308.
- Scudeller, L. A., Mavropoulos, E., Tanaka, M. N., Costa, A. M., Braga, C. A. C., López, E. O., Mello, A. & Rossi, A. M. (2017). Effects on insulin adsorption due to zinc and strontium substitution in hydroxyapatite. *Materials Science and Engineering C*, 79, 802-811.
- Shepherd, J. H., Shepherd, D. V. & Best, S. M. (2012). Substituted hydroxyapatites for bone repair. *Journal of Materials Science: Materials in Medicine*, 23(10), 2335-2347.
- Spicer, P., Kretlow, J., Young, S., Jansen, J. A., Kasper, F. K. & Mikos, A. G. (2012). Evaluation of bone regeneration using the rat critical size calvarial defect. *Nature Protocols*, 7(10), 1918-1929.
- Su, X., Sun, K., Cui, F. Z. & Landis, W. J. (2003). Organization of apatite crystals in human woven bone. *Bone*, 32, 150-162.
- Tite, T., Popa, A. C., Balescu, L. M., Bogdan, I. M., Pasuk, I., Ferreira, J. M. F. & Stan, G. E. (2018). Cationic Substitutions in Hydroxyapatite: Current Status of the Derived Biofunctional Effects and Their In Vitro Interrogation Methods. *Materials*, 11(11), 2081.
- Valenzuela, F., Covarrubias, C., Martínez, C., Smith, P., Díaz-Dosque, M. & Yazdani-Pedram, M. (2012). Preparation and bioactive properties of novel bone-repair bionanocomposites based on hydroxyapatite and bioactive glass nanoparticles. *Journal of Biomedical Materials Research Part B: Applied Biomaterials*, 100B(6), 1672-1682.
- Valiense, H., Barreto, M., Resende, R. F., Alves, A. T., Rossi, A. M., Mavropoulos, E., Granjeiro, J. M. & Calasans-Maia, M. D. (2015). In vitro and in vivo evaluation of strontium-containing nanostructured carbonated hydroxyapatite/sodium alginate for sinus lift in rabbits. *Journal of biomedical materials research. Part B, Applied biomaterials*, 104(2), 274-282.
- Wang, P., Zhao, L., Liu, J., Weir, M. D., Zhou, X. & Xu, H. H. K. (2014). Bone tissue engineering via nanostructured calcium phosphate biomaterials and stem cells. *Bone Research*, 2, 14017.
- Winkler, T., Sass, F. A., Duda, G. N. & Schmidt-Bleek, K. (2018). A review of biomaterials in bone defect healing, remaining short comings and future opportunities for bone tissue engineering. *Bone and joint research*, 7(3), 232-243.
- Yatongchai, C., Placek, L. M., Towler, M. R. & Wren, A. W. (2015). Effects of Strontium Substitution on Bioactivity of Hydroxyapatite. *41st Annual Northeast Biomedical Engineering Conference (NEBEC)*, 1-2.
- You, J., Zhang, Y. & Zhou, Y. (2022). Strontium Functionalized in Biomaterials for Bone Tissue Engineering: A Prominent Role in Osteoimmunomodulation. *Frontiers in Bioengineering and Biotechnology*, 10, 1-22.